INVESTIGATION OF SPECIFIC WHEEL-TERRAIN INTERACTION ASPECTS USING AN ADVANCED SINGLE WHEEL TEST FACILITY

P. Oettershagen[(1)], T. Lew[(1)], A. Tardy[(1)], S. Michaud[(1)]

[(1)] RUAG Space, Schaffhauserstrasse 580, 8052 Zurich, Switzerland, philipp.oettershagen@ruag.com

ABSTRACT

Successful planetary exploration rover missions require high locomotion performance and reliability. However, as experienced by NASA's Mars Exploration Rovers, slip-sinkage events can cause complete immobilization. Accurate locomotion performance prediction via extensive soil-wheel interaction data can reduce such risks. Drawbar Pull (DP) vs. slip tests on Single Wheel Testbeds (SWT) are a common empirical means to collect such data. However, the current literature only covers a limited range of environmental conditions and is thus not fully representative. This paper therefore contributes novel methods and data generated with the RUAG Space SWT facility and the ExoMars Phase B2 wheel: First, drawbar pull measurements on ES-3 soil at negative slip are presented. This is important to assess failed and thus dragging wheels as well as downslope trajectories. It also allows interpolating DP values around 0% slip, which were previously not measurable. Second, a SWT facility that can measure drawbar pull at high slopes is presented. The measurements clearly show that on ES-2, the previous gradability predictions using zero-slope DP data already diverge at >8° slope. The inclined DP measurements are significantly more accurate. ExoMars BB2 rover tests confirm these findings. Both contributions can be used to increase the prediction accuracy of modern locomotion simulator frameworks.

1. INTRODUCTION

Motivation

To design and operate planetary exploration rovers successfully, locomotion performance and reliability prediction is key. However, the incomplete information available to the rover designer (at an early design stage) and rover operator (given missing terrain and soil data) make locomotion performance prediction challenging. As a result, the Mars Exploration Rover (MER) "Opportunity" was stuck twice in loose soil, once for a 30-day period on the "Purgatory Dune" in April 2005, and once for 10 days in June 2006 [1, 2]. MER "Spirit", having suffered a wheel failure in 2006, became fully immobilized in loose soil in January 2010 [3]. These so-called *slip-sinkage* events are "one of the most important failure modes for planetary rovers" [2].

While *a-posteriori* risk mitigation measures such as recovery driving strategies [1], wheel walking [4] and slip-sinkage detection algorithms [5, 6] have been developed, optimally, immobilization risks should be avoided *a-priori*: They should either be mitigated by proper locomotion system design, or should be detectable before entering dangerous terrain. Both approaches require accurate locomotion performance prediction and thus soil-wheel interaction information. A common means to generate this information is drawbar pull testing: The Drawbar Pull (DP), wheel torque and sinkage data is collected as a function of wheel slip, load and soil. This is done either in a rover-level test or, during early design stages, using single wheel testbeds (SWT, Figure 1). Given that drawbar pull testing is *fully empirical*, it is very accurate as long as the test conditions (wheel, soil, environment) are representative. However, most existing literature and projects – due to budget or time constraints – assess these properties under a limited range of conditions such as positive slip and zero terrain slope. As this paper will show, this introduces significant errors into rover-level modeling tools that use such data.

Goal and Contributions

To increase the performance prediction accuracy for rover locomotion systems, this paper supplies novel single wheel test methods and data. The data includes the

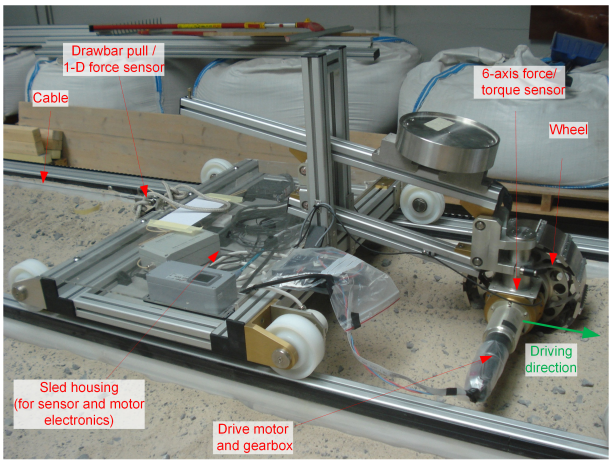

Figure 1: The RUAG Space single wheel test bed in its conventional configuration, i.e. measuring at positive slip and slope=0° in constant-slip mode. This paper presents extensions enabling single wheel drawbar pull testing over a wider envelope, more specifically at negative slip and on steep slopes.

drawbar pull, wheel torque and sinkage of the ExoMars BB2 wheel on ESA's ES-2 and ES-3 soils and represents an accurate fully-empirical soil-wheel interaction model. The data can be used in rover-level simulation tools such as [7]. The specific contributions are:

- *Drawbar Pull SWT testing at negative slip.* Negative slip appears either when a rover descends a slope or when drive train failure causes a blocked and thus dragging wheel. However, most existing literature only covers DP data for positive slips. Formally speaking, this paper extends the common [DP, T, z] = f(soil, load, 0<slip<1) relationship to [DP, T, z] = f(soil, load, -1<slip<1).
- *Drawbar Pull SWT testing on slopes.* The existing literature [2, 8, 9] exclusively discusses single wheel testbeds that measure the drawbar pull at zero degree slope. It is assumed that this DP data can be used to calculate rover gradability, i.e. the maximum slope a rover can climb. This paper investigates this assumption: It presents a single wheel test facility and data for drawbar pull and wheel torque measurements on inclined terrain, and thereby shows that for certain soils, the assumption already breaks down at 8° slope. Formally speaking, this paper extends the commonly identified [DP, T, z] = f(soil, load, slip) relationship to [DP, T, z] = f(soil, load ,slip, slope).

2. FUNDAMENTALS

Soil-wheel interaction mechanics – or terramechanics – are assessed and modeled using three different approaches: First, *continuum mechanics approaches* such as finite element (FEM) or discrete element methods are used to understand and model soil-wheel interaction on a very fundamental level. While accurate and highly versatile with respect to the modeled wheel, soil or rock type, their disadvantage is their computational requirements [10]. Second, the *classical* branch of terramechanics is formed by *semi-empirical* models that focus on modeling the shear stress along the wheel. The foundations for deformable soils (but rigid wheels) were established by Bekker [11]. Extensions were provided by Wong and Reece [12, 13]. Third, *purely empirical* models can be built by experimental testing of representative wheels and soils. Essentially, these methods build large databases of force (drawbar pull), wheel torque and wheel sinkage as a function of wheel slip, wheel load and soil type. The disadvantage is their limited flexibility: While interpolation between the measurements (e.g. wheel load) is possible [7], extrapolation is much more restricted. This already has to be considered during the design of the respective measurement campaign. The main advantages are, first, low computation requirements given that only a look-up table has to be called and, second, high accuracy given a properly designed test facility and thorough test execution. Both semi-empirical and fully empirical models are thus heavily used in rover locomotion simulations tools [7, 10, 14, 15].

As a final output, all methods are interested in the wheel force, torque, sinkage and slip as a function of the environment (soil, wheel load and slope). These metrics are described in Figure 2 and the following:

1) The input torque T is the effective moment the drive unit applies on the wheel. It can be combined with the angular velocity in order to determine the required energy, and is thus also used to size the actuator and drive electronics. The input torque T also defines the soil thrust H, i.e. the actual force the wheel exerts on the soil, via the wheel radius r and

$$H = {}^{T}/_{r} \tag{1}$$

2) The motion resistance R is the resulting force acting in the opposite direction of the motion that in case of a wheel moving on a loose soil is composed of:

$$R = R_c + R_b + R_w + R_g \tag{2}$$

R_c = *compaction resistance*
R_b = *bulldozing resistance*
R_w = *wheel internal resistance force that includes hysteresis (flexible wheel)*
R_g = *gravitational resistance*

3) The drawbar pull DP is the net pulling force in the direction of motion and, for driven wheels, is given by

$$DP = \sum_{j=1}^{j=m} \left(H_j - R_j\right) \tag{3}$$

, where j is the number of wheels. The drawbar pull represents the net force a wheel or rover can use to counteract a motion resistance increase, e.g. due to a slope or obstacle. For towed wheels, the drawbar pull (and in fact H and R) is negative and defined by

$$DP = \sum_{j=1}^{j=m} \left(H_j + R_j\right) \tag{4}$$

4) The slip is defined as follows:

$$slip = 1 - \frac{v_x}{v_{\mathrm{whl}}} \tag{5}$$

v_x = *linear velocity [m/s] of rover* (v_{rvr}) *or sled* (v_{sled})
$v_{\mathrm{whl}} = r \cdot \omega_{\mathrm{whl}}$ = *the wheel translational velocity*
ω_{whl} = *wheel rotational velocity in [rad/s]*
r = *wheel radius [m] (undefl. radius for flexible wheels)*

5) The sinkage z is defined as the vertical distance between the undisturbed surface and the bottom of the wheel without grouser (z_0 in Figure 2). The sinkage depends on the soil characteristics as well as the dimension, shape, stiffness and loading of the wheel.

Note that all those values are slip dependent and need to be determined for different operating condition (e.g. wheel load, multipass, etc.).

6) Multipass
- Multipass "0" defines the first wheel run in the undisturbed soil
- Multipass "i" defines the wheel run when i passes were made before

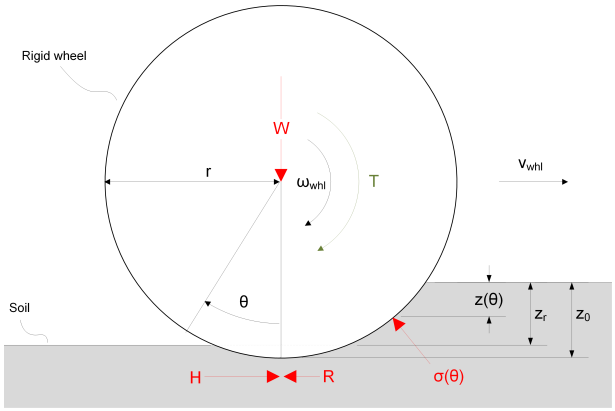

Figure 2: Mechanics of wheel-soil interaction. Forces and pressures (σ) are drawn in red, torques in green.

3. DRAWBAR PULL AT NEGATIVE SLIP

Negative slip occurs when the rover speed v_{rvr} is higher than the linear velocity of the wheel v_{whl}. Having exact locomotion data at negative slip helps predicting locomotion performance in three cases:

- A partially or fully dragging wheel, e.g. due to a drive train failure. This is a critical situation that severely limits locomotion performance and, as happened to MER "Spirit" in 2010 [2, 3], greatly increases the risk of immobilization. In addition, operators may be interested in halting a wheel on purpose to characterize the soil or to uncover scientifically interesting features below the surface.
- When driving downslope. Here, negative slip data clearly helps to predict the movement and exact rover velocity more accurately.
- When descending from objects, e.g. in the crucial phase when the rover needs to descend from its landing platform or when descending with the rear wheels from large rock obstacles.

3.1. Test Setup

Drawbar pull tests are performed in the RUAG Space single wheel test bed [9] shown in Figure 1. For non-inclined (in contrast to Section 4) DP tests, the test bed is conceptually equivalent to existing SWT setups [2, 8] that measure in so called *constant-slip mode* (where slip is enforced, and DP is measured): The wheel is driven through a motor and gearbox mounted through a 6-axis force/torque sensor. Its load is adjusted via a ballast mass. The wheel is attached to a movable sled, which features a cable including a 1D force sensor to measure the wheel's drawbar pull. The cable is extended or retracted at velocity v_{sled} via a motor that is fixed to the testbed. Both v_{sled} and the wheel rotational speed ω_{whl} are measured through encoders. Overall, this *conventional constant-slip* approach is simple and accurate. The only parasitic effect is the sled drag force, which is usually small (a couple of Newtons) and relatively constant versus speed. It is thus simply subtracted from the force sensor measurements.

Figure 1 shows the SWT in the positive slip configuration: Here, $v_{sled} < v_{whl}$ applies, i.e. the wheel is "held back" by the cable. The process to measure negative slip is simple: The rotation direction of the wheel is reversed (which, depending on grouser design, might require to mount the wheel in reverse direction), and the sled or cable speed v_{sled} is increased to now "pull" the wheel such that $-v_{sled} < -v_{whl}$ (which implies $|v_{sled}| > |v_{whl}|$) holds. In both cases, to vary the slip, the wheel speed is constant while the sled speed is adapted.

Table 1: Parameters for DP testing at negative slip.

Parameter	Value
Soil type	ES3-SS3590G
Wheel type	ExoMars Phase B2 wheel
r (wheel radius)	0.125m
v_{whl}	11mm/s
W_{whl} (wheel load)	70N, 180N, 300N

3.2. Results

Figure 3 shows the drawbar pull, wheel torque, resistive force and sinkage results received for slip = $[-100\%, 100\%]$ and the settings in Table 1. All metrics scale with the wheel load. This is expected because the shear force transmittable through the wheel-soil interface changes with the wheel load. The graphs also show a common issue of DP testing with sleds: Given that the sled has a resistive force R_{sled}, no DP values (and thus also no slip) below R_{sled} can usually be measured. In Figure 3, this fact is represented by data gaps around DP=0. They can also not be extrapolated because of the high non-linearity of DP in that region. The advantage of having both negative and positive DP measurements is that this region can, as shown in Figure 3 via 5th order polynomials, easily be interpolated. The resulting graph allows to confirm the expected results that, first, even at DP=0 a slip>0 is required to overcome the wheel resistive force R, and second, to reach slip=0 a slight negative DP (e.g. by driving down a slope) is required.

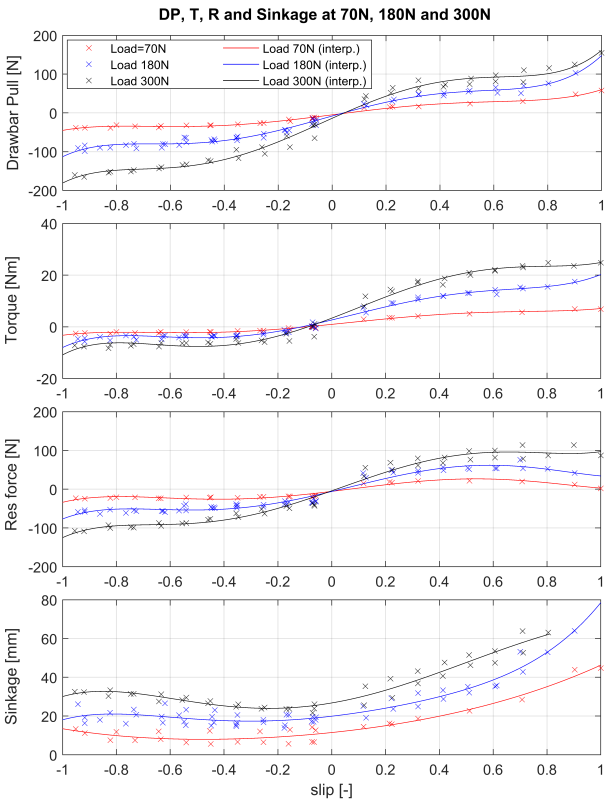

Figure 3: Drawbar pull, wheel torque, resistive force and sinkage measurements for negative and positive slip on ES-3 soil at three different wheel loads.

In addition, Figure 3 shows that the drawbar pull is relatively symmetric around the DP=0 point. Its magnitude is however larger for negative slips because, while R is subtracted from H in the slip>0 case, R acts on top of H (both against the wheel motion) in the slip<0 case. The wheel torque T is not symmetric given that as a driven wheel, the resistance torque needs to be overcome, whereas as a towed wheel it helps to decrease the required motor torque. The resistive force R is symmetric. This is expected because the compaction resistance does not depend on the motion direction (but mainly load and soil type), the resistance due to wheel flex also mainly depends on the load, and the gravitational resistance is negligible on flat soil. The bulldozing resistance mainly depends on the amount of soil that needs to be moved. This is a function of the relative velocity between wheel surface and soil, which, according to Equation (5), is the same for slips of the same magnitude between [-1…1] and v_{whl}=const. Of course, the difference in sinkage between slip>0 and slip<0 might cause changes in the resistive force. The sinkage itself is, as expected, not symmetric but larger for slip>0. All this data helps to model the rover velocity or power consumption over varied terrain much better.

4. DRAWBAR PULL ON NON-ZERO SLOPES

4.1. Test Setup Overview

While conventional single wheel test setups [2, 8], exemplarily shown in Figure 1, are relatively simple concepts that can measure in *constant slip mode,* this situation changes for inclined setups (Figure 5). In addition to the sled drag force R_{sled}, the sled is now subject to the downslope force that (as e.g. in the case of the 52kg RUAG Space SWT sled) significantly limits the measurement range of the test bed or even exceeds the drawbar pull of the wheel. The resulting downslope force thus needs to be compensated either by

- using a closed-loop cable force controller that imposes a given force by adjusting the cable speed.
- manually using a ballast or counter weight W_{ctr} (see Figure 5) that, through a pulley, applies a constant counter force on the cable. This option was chosen due to its simplicity and reliability.

Setting the counter weight

The counter weight W_{ctr} compensates the downhill-slope and resistive forces on the sled. Furthermore, as shown in Equation (6), we can fine-tune it to set the exact drawbar pull that the wheel slip shall be measured at! In contrast to Section 3, this approach is thus measuring in *constant force* (instead of *constant-slip*) *mode* and the slip is only measured via the sled and wheel encoders. For a steady-state motion, the drawbar pull is

$$DP = (W_{sled} + W_{whl}) \cdot sin(\alpha) + R_{sled} - W_{ctr}\,. \quad (6)$$

Here, W_{sled} is the weight of the sled determined via $W_{sled} = m_{sled} \cdot g$ (e.g. through a simple mass measurement), W_{whl} is the wheel load (190N in our case), and the slope angle is α. The sled drag or resistive force is R_{sled}. It is measured under the sled load W_{sled}, at the same speed v_{sled} as used during the later drawbar pull tests but (as an approximation) at zero slope.

While Equation (6) is used to give initial estimates for the required counter weight W_{ctr} and the resulting DP, a direct measurement method was finally applied to avoid any remaining errors in estimating the components of Equation (6). As indicated in Figure 4 and Figure 7, this involves a manual measurement of the resulting drawbar pull DP_{manual} while the sled is pulled upslope at the representative velocity v_{sled}. The counter weight W_{ctr} can then be adjusted iteratively with high accuracy to reach exactly the desired drawbar pull.

An important lesson learned is: The applied DP_{manual} measurement needs to be performed when the wheel is not in contact with the soil (Figure 4), whereas during the final DP measurement the wheel *is* in contact with the soil (Figure 5). Therefore, a change in sled load and thus in sled resistive force occurs such that $R_{sled} = \mu \cdot$

($W_{sled} + W_{whl}$) for the former and $R_{sled} = \mu \cdot W_{sled}$ for the latter case. For the configuration in this paper, the difference in R_{sled} is 27% or, as measured, 6N. This difference is simply added to the desired DP, i.e. if one wants to measure the wheel at DP=20N, then the measurement shall be DP_{manual}=20N+6N=26N.

The advantage of this counter weight method is that a very large range of DPs can be tested: Negative DP and thus slips are achieved by choosing a large W_{ctr}, DP=0 and thus slip~0 are achieved by exactly balancing the downhill-slope and resistive forces via Equation (6), and large positive drawbar pulls (up to the downhill-slope force of sled and wheel) and thus slips are achieved by choosing a small counter weight W_{ctr}.

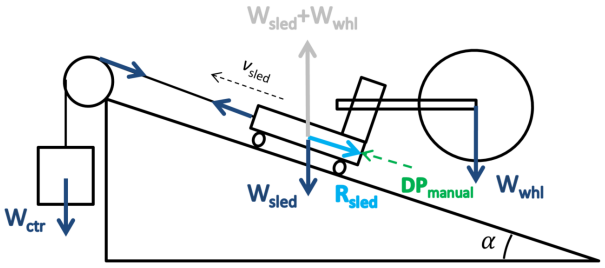

Figure 4: Inclined single wheel testbed in calibration mode, i.e. with the wheel removed from the soil and the force measurement device attached to measure and thereby adapt the current drawbar pull DP_{manual}.

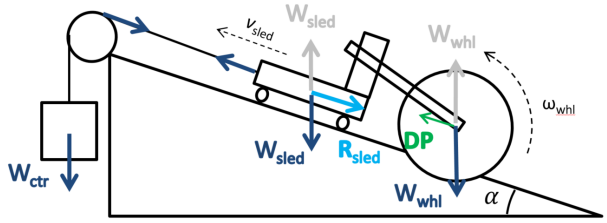

Figure 5: Inclined single wheel testbed in measurement mode, i.e. with the wheel traversing over the soil surface at constant DP such that the resulting slip can be measured.

Figure 6: Tilted SWT at large slopes exhibiting high wheel sinkage. The soil below the motor was partially removed to avoid motor-soil contact.

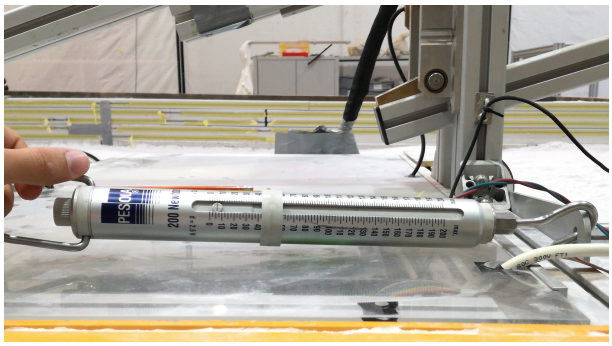

Figure 7: Measurement of the applied drawbar pull DP_{manual} that the wheel will be measured at, shown for slope=6°.

4.2. Test Procedure

The test parameters are summarized in Table 2. The test procedure applied for all tests is as follows:

- Prepare soil, which includes flattening and density verification. For large slope angles where large slip and thus wheel sinkage occurs, it is necessary to remove soil below the motor (Figure 6).
- Clean the Kanya profiles on which the sled wheels move, thereby removing sand or dust which may alter the resistive force R_{sled}.
- Tilt the SWT and measure DP_{manual}, i.e. the force required to move up the slope (see previous section and Figure 7). Iteratively adjust the counter weight W_{ctr} to obtain the desired drawbar pull.
- Start test run with wheel velocity ω_{whl}, and measure the slip by evaluating the linear sled speed v_{sled}.
- Stop the test after 1.5m of driving distance. If excessive slip-sinkage occurs, stop the test, manually set the slip to 100% in the test logs, and label it as "not passed".

Table 2: Test parameters for inclined SWT testing.

Parameter	Value
Soil type	ES-2
Wheel type	ExoMars Phase B2 wheel
v_{whl}	11mm/s
r (wheel radius)	0.125m
W_{whl} (wheel load)	190N
Slopes	0 – 12.7 deg
Driving length	1.5m (less for very high slip)

While this SWT setup supports various combinations of wheel loads and drawbar pulls, a simplified approach was chosen because the main goal was merely to investigate the difference in the predicted gradability based on zero-slope DP and inclined-slope DP data. First, the quasi-static assumption $dv/dt = 0$ leveraged in many rover simulation tools [7] was assumed to also hold on wheel level. In that case, a wheel needs to generate

$$DP = W_{whl} \cdot sin(\alpha) \qquad (7)$$

to maintain its motion on a constant slope α at wheel load W_{whl}. This is exactly the drawbar pull that the SWT was then configured for. When extrapolating the results to rover-level (see Section 4.4), it thus needs to be considered that wheel load changes due to the pitch of the rover are not considered.

4.3. Results

To verify the *constant-force* testing methodology used in this paper against the commonly used *constant-slip*, the setup in Figure 5 was configured to a slope $\alpha = 0°$ and the wheel rotation direction was reversed ($v_{\mathrm{whl}} = -11\,^{\mathrm{mm}}/_{\mathrm{s}}$). Figure 8 shows that the constant-force results agree well with the constant-slip results from previous tests and the overall test setup accuracy is thus confirmed.

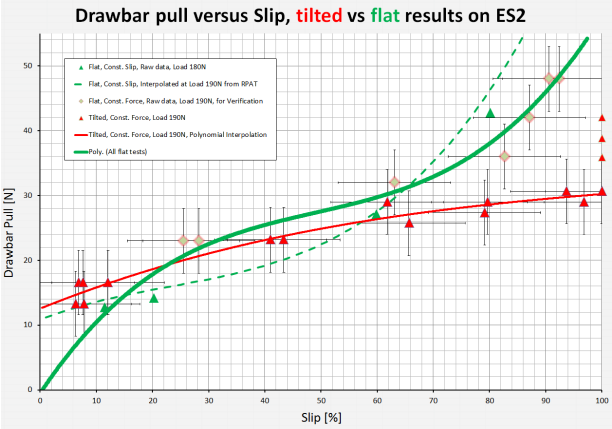

Figure 8: Drawbar pull vs. slip for ES-2 on flat terrain (green) and inclined terrain (red), clearly showing the decrease in drawbar pull on larger slopes (those causing slip>70%). The error bars indicate the measurement uncertainties.

The comparison between drawbar pull for flat (green) and inclined terrain (red) is also shown in Figure 8. Note that for the red curve, the DP is not shown at a constant slope, but at a varying slope (derived via Equation (7), i.e. high DP and slips also represent a higher slope). At low slip (and thus shallow slope) the difference is small. At high slip (and slope angle), the graph however clearly shows that significantly more slip is required to reach a certain DP than predicted by flat-terrain SWT tests. In addition, in some cases the sinkage on the inclined SWT kept increasing over the test length, so the test was stopped to avoid damage to the drive unit and the recorded slip was manually set to 100%. The implications for rover performance are significant: Previous flat-terrain DP testing indicated that a significant drawbar pull reserve is available to scale steep slopes when one allows large wheel slip. However, our results clearly show that this is not the case, i.e. the available drawbar pull reserves are much lower.

This is confirmed by Figure 9, which directly plots the slope (derived via Equation (7)) vs the slip. The difference is again apparent at large slopes. All in all, while flat-terrain DP testing predicts that a slope of around 16° can be climbed if a slip of 90–95% is allowed, the inclined DP test show that only a 9° slope can be negotiated. For rover missions, this means that slope gradability cannot be assessed based on DP tests (whether wheel or rover-level) performed on flat terrain.

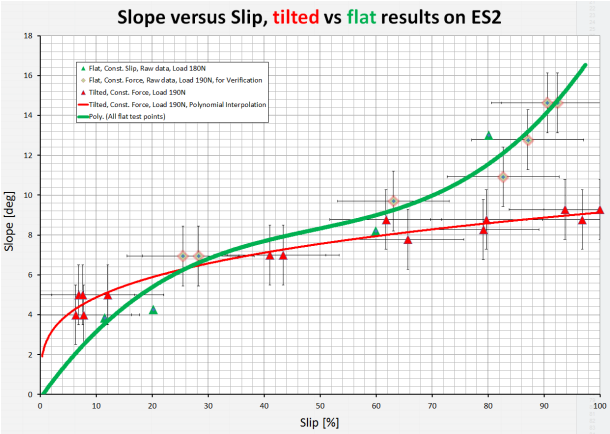

Figure 9: Gradability, i.e. the slope that can be climbed for a certain slip, predicted using common flat-soil SWT tests (green) and using the inclined SWT (red) presented in this paper.

4.4. Comparison to rover-level results

The SWT results were also confirmed via gradability tests with the ExoMars Phase B2 rover (Figure 10). The simulation using the Rover Parametric Analytical Tool [7] using zero-slope DP vs. slip data (green curve in Figure 8) predicts that slopes up to 20° can be climbed on ES-2. However, the rover actually only climbs a 10° slope. This agrees with the 9.5° predicted using inclined SWT tests in Figure 9. Note that small discrepancies between rover measurements and predictions using inclined SWT data are expected because the latter (and thus Figure 9) effectively assumes an even distribution of the rover weight on the wheels, whereas in reality the rear wheels are subjected to higher loads due to the rover tilt.

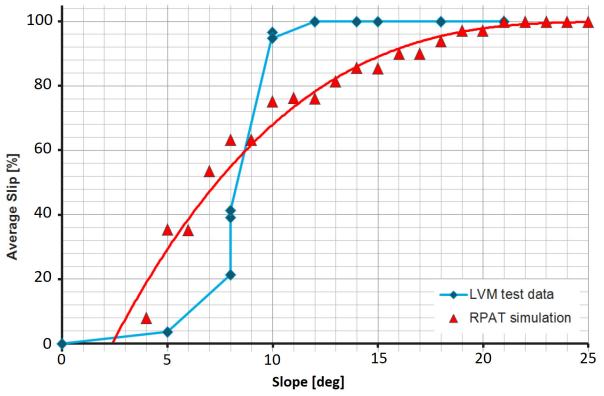

Figure 10: ExoMars Phase B2 rover gradability data vs. predictions using zero-slope DP data.

4.5. Discussion

While a comprehensive analysis requires detailed modelling or experimental investigation via Shear Interface Imaging Analysis [8], visual observations allow a preliminary explanation for the DP difference: For a test at 0° slope and DP=36N (Figure 11), the soil stays flat and does not show a cavity around the wheel. In contrast, even at a lower DP of 31N, the test at 9.6° slope (Figure 12) shows that the wheel rotation creates large cavities at the front and side of the wheel. The cavity's shape is determined by the soil's angle of repose [16].

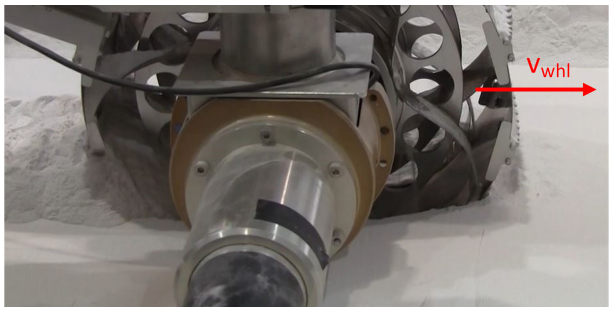

Figure 11: Wheel-soil interaction at DP=36N and 0° slope.

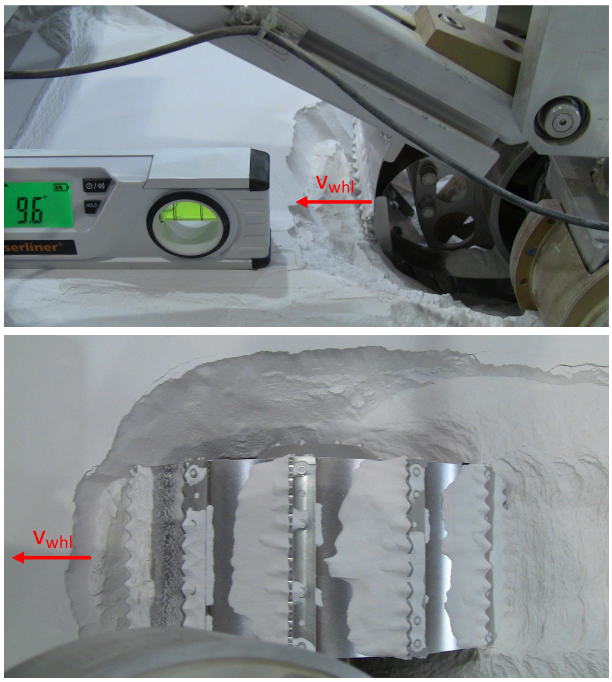

Figure 12: Wheel-soil interaction at DP=31N and slope = 9.6°, clearly showing a cavity characterized by the soil angle of repose in front of and at the side of the wheel.

Figure 13 shows a simplified visualization that partially explains the cavity and reduced drawbar pull. Overall, gravitational effects encourage downslope movement of soil, thus removing soil around the wheel and reducing the effective contact area of the wheel. This effect is particularly pronounced in zone b) of Figure 13, where — due to the high wheel-soil contact pressure σ — gravity and wheel/grouser digging activity quickly remove soil. The wheel sinkage increases, but the removed soil is also continuously replaced from the side and the front (zone a) of the wheel. As a result, cavities at the soil angle of repose [16] form. The cavity in zone a) has significant influence on the drawbar pull: First, it reduces the contact area to transmit shear stress. Second, in contrast to flat terrain, the front grouser (which now enters the soil tangentially to the surface, and not normal to it) and wheel cannot compress the soil anymore. Third, when the angle of repose is exceeded, soil spontaneously flows into the wheel cavity from the front, effectively reducing the relative velocity between wheel and soil (which is equivalent to a slower turning wheel and thus reduces DP). The overall effect is that at the soil-wheel interface, only relatively loose soil is available for force generation. The situation is aggravated because at the rear (zone c), only a weak soil reflow into the wheel cavity exists. This again decreases the contact area and thus drawbar pull. In contrast to the rigid wheel drawn in Figure 13 a flexible wheel helps to limit the reduction in contact area, but the overall mechanics stay the same.

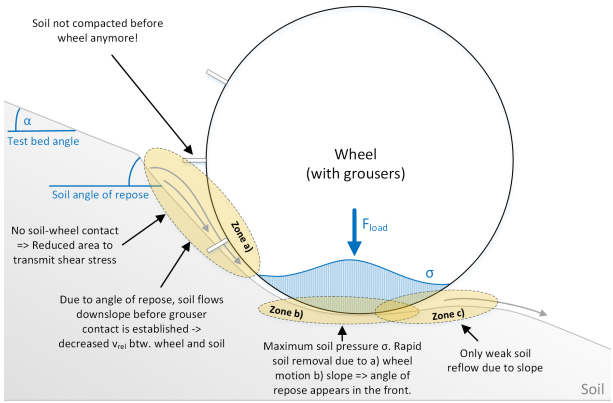

Figure 13: Simplified soil-wheel interaction on inclined terrain and the main differences to flat terrain. For simplicity, a rigid wheel is shown.

5. CONCLUSION

This paper has presented single wheel test (SWT) methods that allow to gather soil-wheel interaction data in two regimes not yet extensively covered in existing literature: First, for the ExoMars Phase B2 wheel on Martian soil simulant ES-2, drawbar pull (together with torque, resistive force and sinkage) test results at negative slip are presented. The results help to model rover motion near 0% slip, when a wheel fails and thus drags, or when the rover is descending slopes, rocks or its own landing platform. Second, while today single wheel drawbar pull tests are mostly done on flat soil and are then extrapolated to assess gradability, the paper clearly shows that this is not admissible. On ES-2, the presented inclined-testbed measurements already show a significant reduction of drawbar pull at >8° slope. Tests with the ExoMars BB2 rover, where the extrapolated drawbar pull data predicts 20° gradability but the actual rover demonstrated only

10° gradability, clearly confirm these results. The advantage of the presented methods and datasets is that they extend existing drawbar pull vs. slip databases while keeping their structure intact. The accuracy of existing rover locomotion simulators can thus be increased without sacrificing their computation speed benefits.

6. ACKNOWLEDGEMENTS

The authors acknowledge that the ExoMars B2 wheel has been developed in the ESA LSS activity by RUAG Space with prime contractor Airbus UK. The comparison with rover level tests has been done with data produced during the ESA LVM activity with prime contractor Airbus UK, using a rover breadboard proprietary to DLR. The tests reported in the paper have been done mainly in parallel to ESA related activities such as UNDERSTAND.

7. REFERENCES

[1] K. Young, "Mars rover escapes from the "Bay of Lamentation"," 2006. [Online]. Available: https://newscientist.com/article/dn9286-mars-roverescapes-from-the-bay-of-lamentation.html.

[2] L. Ding, D. Zongquan, H. Gao, K. Nagatani and K. Yoshida, "Planetary rovers' wheel–soil interaction mechanics: new challenges and applications for wheeled mobile robots," *Intelligent Service Robotics,* pp. 17-38, 2011.

[3] G. Webster and D. Brown, "Now a stationary research platform, NASA's Mars rover Spirit starts a new chapter in red planet scientific studies," 2010. [Online]. Available: http://marsrovers.jpl.nasa.gov/newsroom/pressreleases/20100126a.html.

[4] N. Patel, R. Slade and J. Clemmet, "The ExoMars rover locomotion subsystem," *Journal of Terramechanics,* vol. 47, pp. 227-242, 2010.

[5] M. Bajracharya and e. al., "Autonomy for Mars Rovers: Past, Present, and Future," *Computer,* vol. 41, no. 12, pp. 44-50, 2008.

[6] R. Gonzalez and K. Iagnemma, "Slippage estimation and compensation for planetary exploration rovers. State of the art and future challenges," *Journal of Field Robotics,* vol. 35, no. 4, pp. 564-577, 2017.

[7] P. Oettershagen and S. Michaud, "Development and Validation of a Modular Parametric Analytical Tool for Planetary Exploration Rovers," in *International Symposium on Artificial Intelligence, Robotics and Automation in Space*, 2012.

[8] M. Scharringhausen, D. Beermann, O. Krömer and L. Richter, "Single Wheel Tests for Planetary Applications at DLR Bremen," in *11th European Regional Conference of the International Society for Terrain-Vehicle Systems*, Bremen, Germany, 2009.

[9] S. Michaud, P. Oettershagen and T. Oechslin, "Wheel Level Test Data Generation and Utilization to Predict Locomotion Performances of Planetary Rovers and Validate Simulation Tools," in *International Symposium on Artificial Intelligence, Robotics and Automation in Space*, 2012.

[10] F. Zhou, R. E. Arvidson, K. Bennet, B. Trease, R. Lindemann, P. Bellutta, K. Iagnemma and C. Senatore, "Simulation of Mars Rover Traverses," *Journal of Field Robotics,* vol. 31, no. 1, pp. 141,160, 2014.

[11] M. Bekker, Introduction to Terrain-Vehicle Systems, Ann Arbor, USA: The University of Michigan Press, 1969.

[12] J. Y. Wong, Theory of Ground Vehicles, 4th ed., New York: Wiley, 2008.

[13] J.-Y. Wong and A. Reece, "Prediction of rigid wheel performance based on the analysis of soil-wheel stresses part I. Performance of driven rigid wheels," *Journal of Terramechanics,* vol. 4, no. 1, pp. 81-98, 1967.

[14] R. Krenn and G. Hirzinger, "SCM – A Soil Contact Model for Multi-Body System Simulations," in *11th European Regional Conference of the International Society for Terrain-Vehicle Systems*, Bremen, Germany, 2009.

[15] A. Krebs, T. Thueer, S. Michaud and R. Siegwart, "Performance Optimization of All-Terrain Robots: A 2D Quasi-Static Tool," in *International Conference on Robots and Intelligent Systems*, Beijing, China, 2006.

[16] J. Lee and H. J. Herrmann, "Angle of repose and angle of marginal stability: molecular dynamics of granular particles," *Journal of Physics A,* vol. 26, pp. 373-383, 1993.

[17] S. Michaud, G. A. M. Kruse and M. van Winnendael, "Wheel-Soil Interaction Data Generation and Analysis on Characterized Martian Soil Simulants," in *i-SAIRAS*, Beijing, 2014.

[18] S. Michaud, G. A. M. Kruse, M. Karaoulis, D. de Lange and M. van Winnendael, "Sensing Techniques to Characterize Locomotion on Soils to be Traversed by a Rover," in *Proceedings of the 14th ESA Workshop on Advanced Space Technologies for Robotics and Automation (ASTRA)*, Leiden, The Netherlands, 2017.

[19] S. Michaud, G. Kruse, D. de Lange and M. van Winnendael, "Sensing Techniques to Characterize Locomotion on Soils to be Traversed by a Rover," in *ASTRA*, Noordwijk, The Netherlands, 2017.